

A DEM-CFD coupling method in studying scour around a circular pile

L.Q Nguyen-Thi^{1,2}, V.D Nguyen¹, P. Coorevits¹, T.Q Duong², C. Nguyen-Manh²

1. Université de Picardie Jules Verne - Laboratoire des Technologies Innovantes EA 3899, IUT, 48 rue d'Ostende, 02100 Saint-Quentin, France.
Email: quyen.nguyen-le@u-picardie.fr
2. National University of Civil Engineering, 55 Giai Phong street, Hanoi, Vietnam.
Email: cuongnm@nuce.edu.vn

Abstract:

The variability of hydromechanics and physicochemical conditions, as well as the effects of climate change, possibly contribute to the deterioration of construction structures that are located in fluvial and maritime environments. Bridge piers and offshore wind turbine foundations (monopile and suction monopod foundations) are examples of such structures, and local scouring has been identified as one of the main phenomena resulting from the aforementioned conditions. Additionally, bridge failures are associated with scouring and erosion. Although the study of soil erosion and scour formation constitutes a significant challenge, it is critical to acquire an in-depth understanding of these phenomena to enable them to be controlled or prevented altogether. On the one hand, the classical two-phase model of sedimentation utilizing the finite element method needs to be combined with granular rheology and hydrodynamic analysis to estimate bed shear stress on a global scale. On the other hand, physical fluid-particle interaction could be investigated using the discrete element method (DEM). To date, this method becomes an interesting tool allowing us to understand the effects of vortex around foundations and the influence of the bed roughness on local scour. This paper presents a coupling of discrete element method and computational fluid dynamics (a coupled DEM-CFD method), which is validated by experimental sedimentation for one particle and by a confrontation with the literature review of hydrodynamic flow around a circular pile on smooth rigid-bed. Finally, the scour results of a sand bed will be presented.

Keywords: DEM-CFD coupling, scour, particle-particle interactions

1. Introduction

Scour around a circular pile under the impact of currents is state of matter. For the construction structures located in a maritime environment, whose foundations are directionally suffered from flows affected from the variability of hydromechanical and physicochemical conditions, as well as climate change, possibly contribute them to the deterioration. Among the resulting phenomena, local scour has been identified as one of the

main factors. In the United States, over the last 30 years, 60% of over 1000 bridges failures are associated with scouring and erosion (Briaud et al., 1999) [1]. Among offshore wind turbines built on the European coast, a major proportion of these turbines have a monopile platform. Therefore, the understanding of sediment process around a circular pile plays a vital role in predicting scour to design foundations and protection solutions.

Even though numerous experimental and numerical research in the literature, not all physical processes involved are yet well understood and presented. Among these studies, the appearance and the formation of horseshoe vortex in front of the circular pile, the formation of the vortex shedding behind and the generation of turbulence impact to the mechanism of sediment transportation around the structure foundations were investigated. This process is very complex due to in most cases it involves two-phase turbulent flows and various sediment transport modes.

Consequently, in the pioneer study by Roulund *et al.* [2], the authors investigated the rigid-bed experiments with a vertical circular pile in a steady current. The velocity profiles were investigated in the plane of symmetry upstream and downstream of the pile. Then, a scour experiment was conducted in a current flume with a sand pit. The difference in the surface elevation between the front and side edges of the cylinder, the horseshoe vortex caused by the rotation in the incoming flow and the influence of the bed roughness were examined. Recently, Lachaussée *et al.* [3] studied the scour of a sand bed platform around a vertical cylinder submitted to strong enough steady water flow. The authors showed that the classical scour pattern "horseshoe" is observed at the cylinder foot at a critical velocity. When the velocity becomes smaller, two symmetrical ovoid holes having "bunny ears" shape due to wake vortices, were observed.

From a numerical point of view, classical sediment transport models depend on the empirical formula for the bed-load and suspended-load governed by Exner equation [4,5]. In large scale, bed level change in computational fluid dynamics (CFD) needs to be interpolated from computational morphodynamics [3, 6]. Over the last decade, the modeling of sediment transport using two-phase flows has developed at the intermediate scale. This approach is based on the solution of momentum and mass conservation equations for each phase: liquid and particle. The sediment shear stress is modeled using frictional rheology of granular media [7-9].

Recently, the sediment saltation in a rough-wall turbulent boundary layer was simulated with a coupled model with Large Eddy Simulation (LES) and a Discrete Element Model (DEM) [10]. The two-way coupled model by a DES-DEM (Detached Eddy Simulation) of bridge local scour behavior was investigated by Li *et al.* [11]. The authors observed that the scour was initiated upstream of the pier by the dynamic horseshoe vortex, where the maximum scour depth occurred.

This paper aims at presenting a coupled DEM-CFD method that takes into account the particle-particle collisions and the solid-fluid interactions on the local granular scale. This coupling model is validated by experimental sedimentation for one particle and by a confrontation with the literature review of hydrodynamic flow around a circular pile on smooth rigid-bed. Finally, the scour results of a sand bed will be presented.

2. A DEM-CFD Coupling

The coupled DEM-CFD model (a process combined the Discrete Element Method and Computational Fluid Dynamics to describe the particle-fluid two-phase flow) in this study based on the Lagrangian scheme adopted for DEM, along with the Eulerian framework for the fluid phase. This DEM-CFD coupling is implemented by the DPMFoam solver in the open source code OpenFOAM [12].

The finite volume method (FVM) technique is used for the CFD, the mesh is structured, and the size mesh is much larger than the particle size (Fig. 1). The fluid in the CFD is described by locally averaged Navier-Stokes equations:

$$\rho \frac{\partial \varepsilon U}{\partial t} + \rho \nabla \cdot (UU) - \rho \nabla \cdot \varepsilon \tau = -\nabla p + \rho \varepsilon g - F^f \quad (1)$$

Where ε is the volume fraction, p the fluid pressure, μ the fluid viscosity, ρ the fluid density, g the gravity and τ the stress tensor. The term F^f denotes the effect of particles on fluid motion through the fluid drag force.

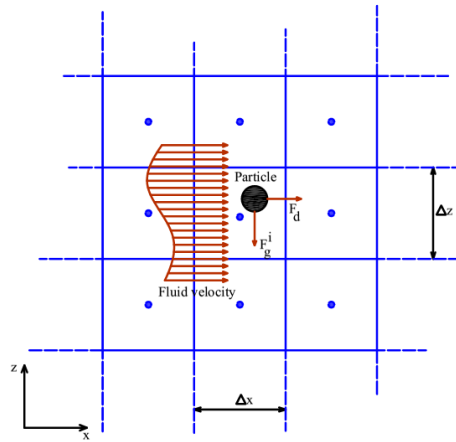


Figure 1: The sketch of forces acting on particles.

The equation of continuity is given by

$$\frac{\partial \varepsilon}{\partial t} + \nabla \cdot (\varepsilon U) = 0 \quad (2)$$

The motion of the discrete particles was governed by Newton's laws of motion [3-5,13] :

$$m_i^P \frac{dU_i^P}{dt} = F_{ij} + F_i^f + F_i^g \quad (3)$$

$$I_i = \frac{d\omega_i}{dt} = M_{ij} \quad (4)$$

Where P is noted for the particle, m_i^P , U_i^P and ω_i are the mass, translational and angular velocities of the particle i ; M_{ij} is the contact torque force acting on particle i by the particle j ; F_{ij} is the contact forces acting on particle i by particle j ; F_i^g the gravitational force acting on particle i ; I_i and is the moment inertia of the particle i .

The particle in this work treated as a sphere modeled as soft-sphere. The particle-particle contact forces (Fig. 2) are simulated by the simple spring-dashpot model [13-15]. In this

study, the cohesive force is not taken into account; the coefficient of restitution is 0.98 and the friction coefficient is 0.1.

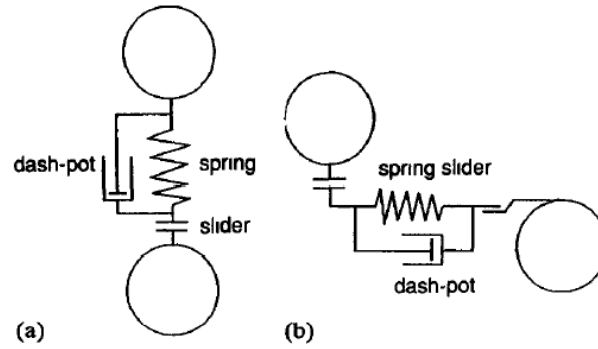


Figure 2: Models of contact forces: (a) normal force; (b) tangential force.

Particles in the fluid environment will have been contacted with fluid flow surrounding them, which will result in several particle-fluid interaction forces such as pressure gradient force, lift force, drag force, etc. This work first studies fluid-particle contact drag force (F_d) acting on particles (Fig. 1) to validate the coupled DEM-CFD method, other forces (pressure gradient force, lift force) will be investigated and integrated later.

The drag force is given as the equation below:

$$F_D = C_D \frac{\pi d_p^2}{8} \rho |U^f - U_i^p| (U^f - U_i^p) \quad (5)$$

The drag coefficient C_d is adopted from Schiller-Naumann (1935) [16]:

$$C_d = \begin{cases} \frac{24}{Re_p} (1 + 0.15 Re_p^{0.678}), & \text{if } Re_p \leq 1000 \\ 0.44, & \text{if } Re_p > 1000 \end{cases} \quad (6)$$

3. Validation and results

3.1. Validation of DEM-CFD coupling

3.1.1. Sedimentation of one particle

The validation is complemented by comparison with the experiment's results of ten Cate *et al.* (2002), [17]. In this study, the objective was to accurately measure both the trajectory (position as a function of time) and the associated flow field of a settling sphere. The parameters of the particle are illustrated in Table 1. The two cases are correspondent with two types of the characteristic of fluid as shown in Table 2. The container dimensions were chosen as $depth \times width \times height = 100 \times 100 \times 160$ mm. The sphere was released from a height of 120 mm to the bottom of the tank (Fig. 3).

Table 1

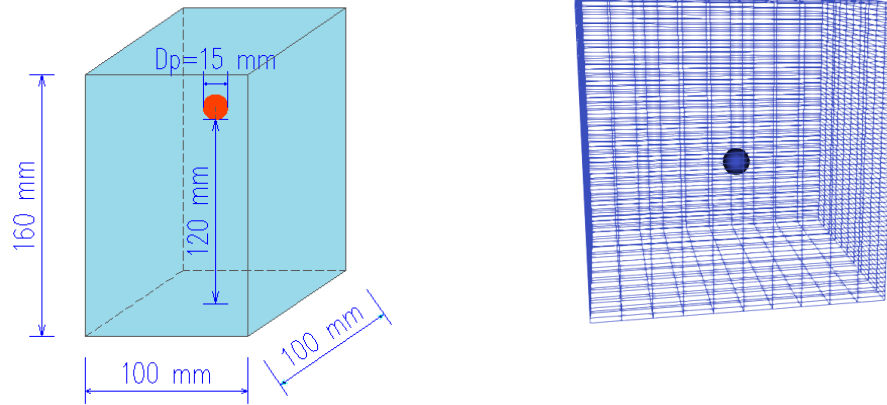
The parameters of the settling sphere particle

The diameter of the particle, d_p [mm]	The density of particle, ρ_p , [kg.m ⁻³]
15	1120

Table 2

The case definition of the experiment for one settling sphere particle

Case number	The density of fluid, ρ_f [kg.m ⁻³]	Dynamic viscosity of fluid, μ_f [N.s.m ⁻²]	Re [-]
1	970	373	1.5
2	960	58	31.9



a) Sketch of the experimental domain setup.

b) Numerical model.

Figure 3: Sedimentation model.**The numerical model description:**

To reduce the effect of boundary conditions, the dimensions of the simulation model was extended to the domain dimension as $depth \times width \times height = 300 \times 300 \times 300$ mm. The distance from the sphere to the bottom of the tank in the numerical model is still unchanged by 120 mm. The size of the mesh is $\Delta x \times \Delta y \times \Delta z = 30 \times 30 \times 5$ mm. The simulation calculation obtained using an absolute tolerance for velocity equal to $1.0E-08$ and zero for the pressure. The time step of convergence Δt equal to $1.0E-04$.

Validation:

Figure 4 shows the comparison of the above-mentioned experimental results in terms of trajectory (panels a, c) and vertical velocity (panels b, d) of the sphere in the two cases of Reynolds number value, 31.9 and 1.5 respectively.

Regarding the first case ($Re = 31.9$), as can be seen from figure 4a, the dimension gap height (z/d_p) over time agrees quite well between experiment and simulation measurements. Nevertheless, the vertical velocity shows part of the difference. Although there is a similar trend, in the numerical model, the sphere starts rising faster than that in the experiment for the 0.28s period from the beginning of the simulational total time. After that, the particle drops back to zero with velocity is nearly constant by approximately 0.093 m/s. This comparison is quite satisfactory; meanwhile, in the experiment model, the particle falls vertically to the bottom with the increasing velocity.

In terms of the low Reynolds number ($Re = 1.5$), there is a relative difference from the simulation compared to experimental results in both trajectory and velocity of the sphere. This disagreement might be caused by the dominant viscous effect in the Stokes regime.

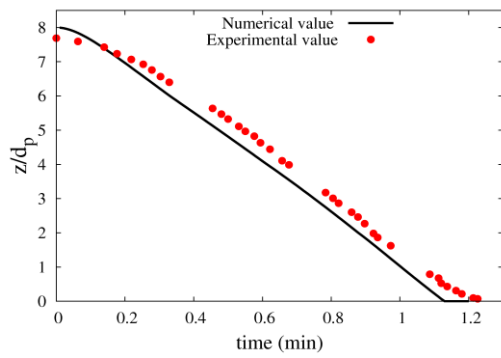
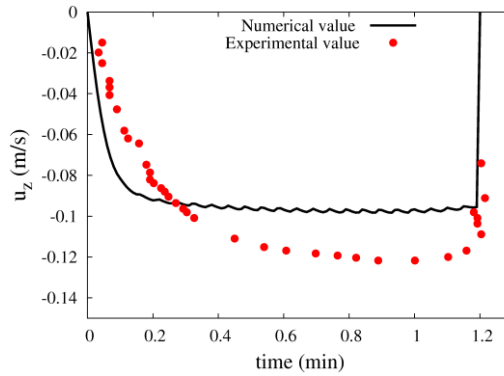
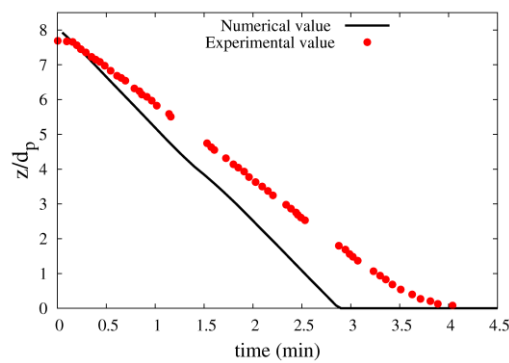
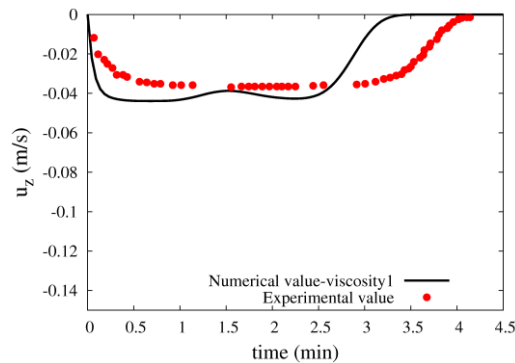
a) Experimental data and the numerical result of sphere trajectory at $Re=31.9$.b) Experimental data and the numerical result of sedimentation velocity at $Re=31.9$.c) Experimental data and the numerical result of sphere trajectory at $Re=1.5$.d) Experimental data and the numerical result of sedimentation velocity at $Re=1.5$.

Figure 4: Comparison between numerical study and experimental data of sedimentation.

3.1.2. Hydrodynamic study of flow around a circular pile on smooth rigid-bed

The hydrodynamics of the DEM-CFD coupling has been validated against the experiment of Roulund *et al.* (2005) for the smooth rigid-bed case [2]. The experiment was conducted with a vertical circular pile in a steady current, in a flume, 35 m long and 3 m wide. The water depth was maintained at 54 cm, and the velocity is at $U_x = 32.6 \text{ cm s}^{-1}$ (Table 3).

Table 3:

The case definition of experiment

Water depth, h	[cm]	54
Mean flow velocity, U_x	[cm.s^{-1}]	32.6
Pile diameter, D	[cm]	53.6
Pile Reynolds number, $Re_{D,V}$	[-]	1.7×10^5

Numerical model:

The numerical was built without particles. The simulation expected time is sixty seconds. The dimension and the mesh characteristics for the domain calculation, as well as the absolute tolerance for the pressure and velocity for convergence after each time step in the numerical model, are summarized in Table 4.

Table 4

Characteristics of the numerical calculation

The depth of calculation domain	D
Length of calculation domain	120D
The width of the calculation domain	80D
Total mesh cells	853,272
Number of cells around the pile perimeter	32
Total simulation time, t_f (s)	60
Time step, Δt (s)	5.0E-05
The absolute tolerance for pressure	1.0E-08
The absolute tolerance for velocity	1.0E-08
The relative tolerance for pressure	0
The relative tolerance for velocity	0.001

Figure 5 shows the mesh in the simulation and the horizontal fluid velocity field at the time of 2.8s, the mesh around the cylinder is refined. As we can see from the velocity field (Fig. 5), the decrease of velocity at the upstream and downstream of the cylinder and the increase on side edges of the cylinder were observed. This is quite satisfactory with the literature review.

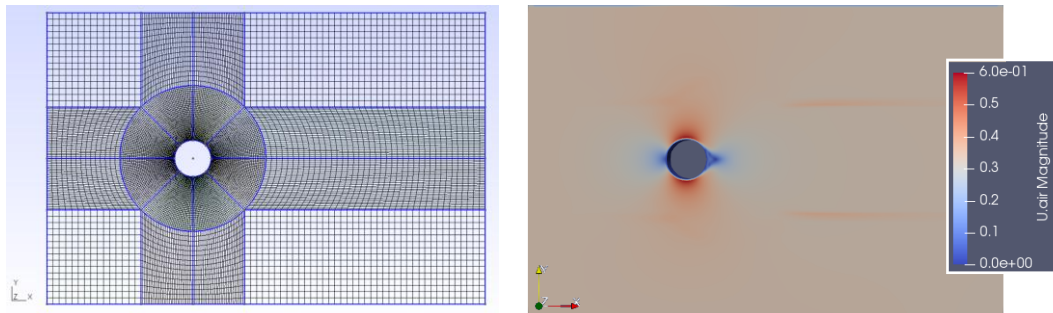
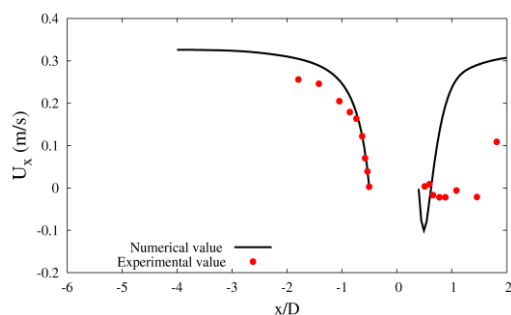
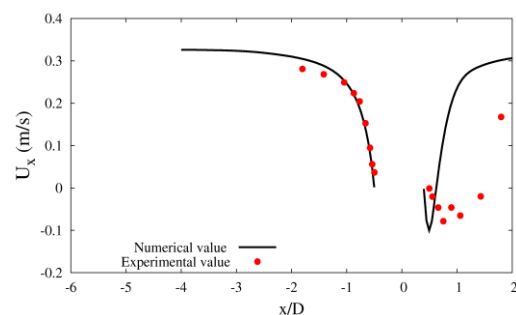


Figure 5: Mesh of numerical model (left) and velocity field (right).

Figure 6a and 6b show the comparison between numerical study and experiment data of the horizontal velocity in the plane of symmetry at time of 2.8s for two values of the distance z from the bed, at $z = 5$ cm and at $z = 10$ cm, respectively. Figure 7c and 7d, on the other hand, show the calculated horizontal velocity besides the pile (at $y = 2.5$ m) at the same distance from the bed.



a) Horizontal velocity, U_x (m/s), in the plane of symmetry at 5cm from the bed.



b) Horizontal velocity, U_x (m/s), in the plane of symmetry at 10cm from the bed.

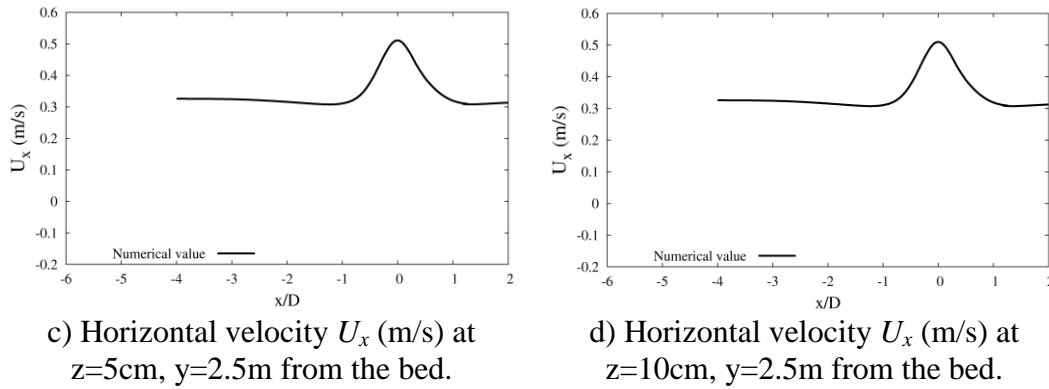


Figure 6: The horizontal velocity profiles at $t=2.8\text{s}$.

As can be seen in Figure 6a and 6b, the graphs of fluid velocity in both numerical and experimental model show a good agreement on the upstream side of the pile. There is still a similar trend in the graph of velocity on the downstream side of the pile despite the different fluid velocity values in two models. This can be due to the simulation time not enough to reach a steady state. In Figure 6c and 6d, the graphs of horizontal velocity indicate that the stability of this flow before and after reaching a peak at about 0.5m/s in the position between the pile and the boundary. This is suitable for the physical fact.

3.2 Scour around a circular pile: Results and discussions

In this part, the experimental study of Lachaussée *et al.* (2017) is inspired [3]. The authors studied the scour of a bed sand surface around a vertical cylinder submitted to strong enough steady water flow. The classical scour pattern "horseshoe" is observed at the cylinder foot at a critical velocity. Main properties of the experimental setup are detailed in Table 5.

Table 5:

The case definition of the experiment of Lachaussée

Domain dimensions, $length \times width \times height$	[mm]	300×600×160
Cylinder diameter, D	[mm]	20
Cylinder Reynolds number, Re_D	[-]	3.6×10^3
Sand layer thickness, δ	[mm]	40
Sand density, ρ_s	[kg.m^{-3}]	2500
Sand diameter, d_s	[μm]	270 ± 30
Fluid velocity, U_f	[m.s^{-2}]	0.16
The absolute tolerance for pressure	[-]	1.0E-06
The absolute tolerance for velocity	[-]	1.0E-05
The relative tolerance for pressure	[-]	0.01
Time step, Δt	[s]	0.1

Simulation model:

The numerical parameters of the simulation model are shown in Table 6. To reduce the calculation by a decrease in the total number of particles, the numerical model is simulated as a smaller size compared with the experiment model.

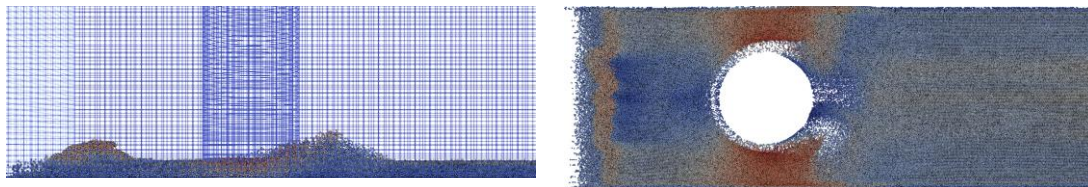
Table 6:

Simulation parameters of the numerical model

Length of calculation domain	[mm]	115
------------------------------	------	-----

The width of the calculation domain	[mm]	40
The depth of the calculation domain	[mm]	90
Total number of particles	[-]	390,500
Number of cells around the pile perimeter	[kg.m ⁻³]	32
Total simulation time, t_f	[s]	5
Time step, Δt	[s]	1.0E-04
The absolute tolerance for pressure	[-]	1.0E-06
The absolute tolerance for velocity	[-]	1.0E-05
The relative tolerance for pressure	[-]	0.01
The relative tolerance for velocity	[-]	0.1

Fig. 7 shows scour formed under the effect of fluid flow and cylinder pile. Quantitatively speaking, the scouring formation in the simulation quite follows of that in experimental results. Scour forms in the front of and behind the cylinder in general and in this first period of simulation time, the scour is gathered much behind compared to the front of the pile.



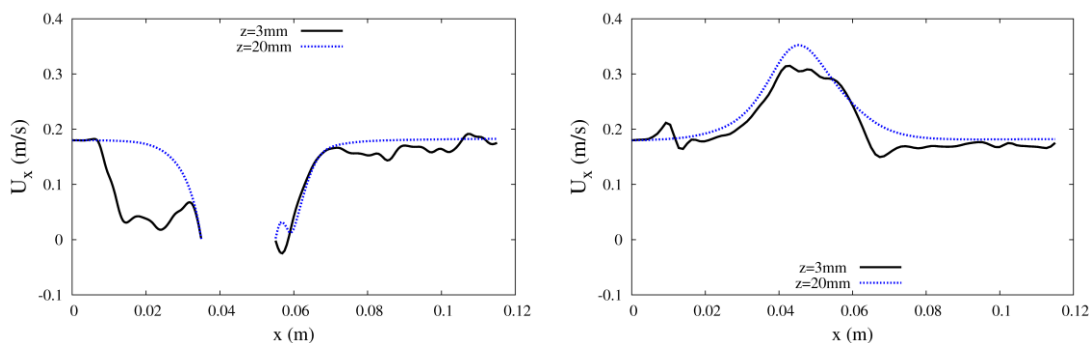
a) Horizontal velocity, U_x (m/s), in the plane of symmetry at 5cm from the bed ($t=0.09s$).

b) Horizontal velocity, U_x (m/s), in the plane of symmetry at 10cm from the bed ($t=0.09s$).

Figure 7: Bed deformation over time at the plane zx intersects the center of the cylinder.

The simulation results:

Figure 8 shows the variation of the horizontal velocity of the fluid in the plane of symmetry and beside the circular pile (at $y=2.5m$) for the differences of z level: $z=3mm$ and $z=20mm$ from the bottom at $t=0.09s$.



a) Horizontal velocity, U_x (m/s), in the plane of symmetry ($t=0.09s$).

b) Horizontal velocity, U_x (m/s), beside the circular pile ($t=0.09s$).

Figure 8: Variation of horizontal velocity on numerical model length.

Take a glance at Fig. 8a, it can be seen that, at the distance $z=3mm$ from the bottom, the velocity fluctuates both before and after hitting the cylinder. At the upstream, after standing at the initial value of 0.18 m/s for about 5mm, fluid velocity decreases dramatically to nearly 0.05 m/s and stands at this value about 10mm before reaching to a peak at approximately

0.05m/s. It almost falls immediately to zero when hitting the cylinder. At this z level, is also on the face of the sand layer; therefore the varying of fluid velocity could explain by the effects of the roughness. All physical phenomenon mentioned above is further confirmed when observing the velocity of water at the height of 20mm. In this level, the velocity of the fluid is no longer affected by roughness so that the velocity is unchanged at 0.18m/s until drops back to zero when it takes a hit to the cylinder. At downstream, the opposite trend is seen to the fluid velocity, and this meets the accordance with the mechanism reported in the literature. In terms of Fig. 8b, a similar principal explanation could be used for the horizontal velocity of fluid besides the cylinder.

The change of fluid velocity over time acting on the change of particle velocity due to the varying of fluid-interaction force exerted on particles. The direction and magnitude of particle velocity change leading to the deformation of different level of the sand bed. This deformation is changed over time until reaching equilibrium. Fig. 9 illustrates the level change of sand bed over 0.09s of simulation period at the downstream of the cylinder.

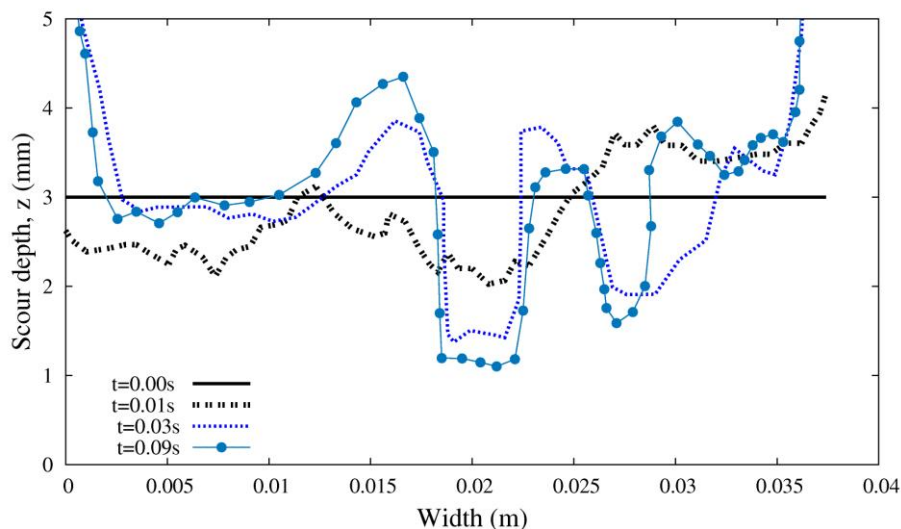


Figure 9: Bed level changes over time.

Conclusions

A coupled DEM-CFD method has been presented to study the scour of sand particles around a circular pile. The interaction between fluid and particle is considered by drag force between the DEM and the CFD. Through two experimental/numerical confrontations, the following conclusions can be made:

- For the case of validation for one particle, the concordance between the experimental and the numerical results was observed for a Reynolds number of 31.9. Yet, there is an insignificant difference between the numerical results and the experiment data in the latter case ($Re=1.5$). The particle in the simulation falls faster than that in the experiment. Further refinement of the present drag model is also in perspective; the effects of viscosity and the Stokes' law will be taken into consideration. Both the hydrodynamics and sedimentation transport in the numerical model still needs rigorous verifications by experiments in steady state in the future.
- For the validation case of scour around a circular pile, the erosion seems to happen faster in the simulation compared to the experiment model. This might be due to the effect of

viscosity; therefore the viscosity of particle-fluid two-phase flow affected by particles in the fluid motion through the drag force has to take into account. Further improvements may be implemented by considering the influence of particle-particle cohesion and the effect of porosity on drag force. The study nevertheless constitutes the first step towards a more expanded model with more particles in steady state.

Références

- [1] J. L. Briaud; Francis C. K. Ting; H. C. Chen; R. Gudavalli; Prediction of Scour Rate in Cohesive Soils at Bridge Piers, 1999. [https://doi.org/10.1061/\(ASCE\)1090-0241\(1999\)125:4\(237\)](https://doi.org/10.1061/(ASCE)1090-0241(1999)125:4(237))
- [2] ROULUND, A., SUMER, B., FREDSE, J., & MICHELSEN, J. (2005). Numerical and experimental investigation of flow and scour around a circular pile. *Journal of Fluid Mechanics*, 534, 351-401. doi:10.1017/S0022112005004507
- [4] Jacobsen, Mass conservation in computational morphodynamics: uniform sediment and infinite availability, *International journal for numerical methods in fluids Int. J. Numer. Meth. Fluids* 2015; 78:233–256 2015, DOI: 10.1002/flid.4015
- [3] Lachaussée F., Yann Bertho1, Cyprien Morize1, Alban Sauret & Philippe Gondret, Motifs d'érosion dans le sillage d'un cylindre, Rencontre du non-linéaire 2017
- [5] Xiaofeng Liu, Numerical models for scour and liquefaction around object undercurrents and waves, Thesis, University of Illinois at Urbana-Champaign, 2008
- [6] Xu, B.H., Yu, A.B., Numerical simulation of the gas-solid flow in a fluidized bed by combining discrete particle method with computational fluid dynamics, *Chem.Eng.Sci.*52,2785–2809 (1997)
- [7] Cheng Z., Hsu T.-J., Calantoni J , SedFoam: A multi-dimensional Eulerian two-phase model for sediment transport and its application to momentary bed failure, (2017) *Coastal Engineering*, 119 , pp. 32-50.
- [8] T. Nagel, J. Chauchat, Z. Cheng, X. Liu, T.-J. Hsu, C. Bonamy, Olivier Bertrand [Two-phase flow simulation of scour around a cylindrical pile](#) (pp. 65-72) - DOI:10.5150/jngcgc.2016.008
- [9] Chauchat, J., Cheng, Z., Nagel, T., Bonamy, C., and Hsu, T.-J.: SedFoam-2.0: a 3-D two-phase flow numerical model for sediment transport, *Geosci. Model Dev.*, 10, 4367-4392, <https://doi.org/10.5194/gmd-10-4367-2017>, 2017.
- [10] Liu D., Liu X. & Xudong Fu (2018): LES-DEM simulations of sediment saltation in a rough-wall turbulent boundary layer, *Journal of Hydraulic Research*, DOI: 10.1080/00221686.2018.1509384
- [11] Li, J., & Tao, J. (2018). CFD-DEM Two-Way Coupled Numerical Simulation of Bridge Local Scour Behavior under Clear-Water Conditions. *Transportation Research Record*, 2672(39), 107–117. <https://doi.org/10.1177/0361198118783170>
- [12] <https://openfoam.org>
- [13] Cundall, P.A., Strack, O., A discrete numerical model for granular assemblies, *Géotechnique* 29(1), 47–65 (1979).
- [14] Tsuji, Y., Tanaka, T., Ishida, T., Lagrangian numerical simulation of plug flow of cohesionless particles in a horizontal pipe, *Powder Technol.* 71, 239–250 (1992)

- [15] Tsuji, Y., Kawaguchi, T., Tanaka, T., Discrete particle simulation of two-dimensional fluidized bed, *Powder Technol.* 77(1), 79–87 (1993)
- [16] Fernandes, C., Semyonov, D., Ferrás, L.L. et al., Validation of the CFD-DPM solver DPMFoam in OpenFOAM through analytical, numerical and experimental comparisons, *Granular Matter* (2018)
- [17] ten Cate A., C. H. Nieuwstad, J. J. Derksen, and H. E. A. Van den Akke, Particle imaging velocimetry experiments and lattice-Boltzmannsimulations on a single sphere settling under gravity, *Phys. Fluids*, vol. 14, no. 11, p. 4012, 2002.